Journal of Thermal Engineering
https://jten.yildiz.edu.tr/
https://doi.org/10.47481/jten.0065

RESEARCH ARTICLE

Enhancing solar evacuated tube receiver performance through environmental isolation with an enclosure

Dheya Ghanim Mutashert[1,*], Lina Jassim[2], Ali Najim Abdullah Saieed[3], Karrar A. Hammoodi[4], Hasan Shakir Majdi[5]

[1]Mechanical Engineering Department, University of Technology-Iraq, Baghdad 10066, Iraq
[2]Mechanical Engineering Department, Mustansiriyah University, Baghdad 10052, Iraq
[3]Department of Refrigeration and Air Conditioning Engineering, Al-Rafidain University College, Baghdad 10014, Iraq
[4]Department of Air-Conditioning and Refrigeration Techniques Engineering, University of Warith Al-Anbiyaa, Baghdad Rd, Karbala, 56001, Iraq
[5]Department of Chemical Engineering and Petroleum Industries, Al-Mustaqbal University College, 51001 Hillah, Babylon, Iraq

Abstract

The research addresses the reduction in performance of solar evacuated tube collectors resulting from environmental conditions, including wind, ambient temperature, and humidity. The thermal efficiency of solar collectors needs to be enhanced to enable the development of more sustainable heating systems. Solar evacuated tubes exhibited improved heat retention through a newly designed, isolated enclosure that protected them from environmental factors. The simulation evaluated the thermal performance of solar evacuated tubes for enclosure gaps of 10 cm, 20 cm, and 30 cm and for tube azimuth angles of 0° and 40°, under summer and winter conditions. The thermal enclosure raised the tube's average maximum internal temperature from 321 K to 328 K, resulting in notable heat accumulation. A 10-cm enclosure gap reached a temperature of 314.5 K at 1:00 p.m., with a thermal efficiency of 94.29%. The designed enclosure prevented heat loss during sunset hours, thereby improving system reliability. Building on previous research, this paper presents an uncomplicated enclosure system that optimizes heat-transfer performance and thermal efficiency using basic design methods that do not require sophisticated tracking equipment. The Results confirm that solar thermal collectors with enclosure systems function as economical and effective methods to enhance performance regardless of environmental conditions.

Keywords: Solar thermal energy, enclosure, heat transfer, integrated pressure, renewable energy, evacuated tube collector, sustainable heating

Cite this article as: Mutasher, D. G., Jassim, L., Saieed, A. N. A., Hammoodi, K. A., & Majdi, H. S. (2026). Enhancing solar evacuated tube receiver performance through environmental isolation with an enclosure. Journal of Thermal Engineering, 12(5), 1778–1797. https://doi.org/10.47481/jten.0065

1. Introduction

Solar energy is the leading sustainable power solution, and solar thermal systems play a critical role. The thermal efficiency of evacuated tube collectors is unstable because environmental factors cause wind effects, heat losses, and temperature variations. Modifying system configurations by adding barriers and vanes inside porous cavities enhances heat-transfer capabilities and improves the distribution of the Nusselt number. This study proposes a new solar evacuated-tube design that reduces heat loss and improves stability using passive methods rather than magnetic fields or nanofluids. Computational analysis indicates improved heat conservation and higher efficiency, providing a passive system design for solar thermal devices suitable for residential and commercial use.

The hybrid model reliably forecasts the average fin temperature during daytime operation and delivers rapid, accurate

*Corresponding Author
E-mail Adress: 20075@uotechnology.edu.iq

Submitted: 2 March 2025; **Accepted:** 21 July 2025

This paper was recommended for publication in revised form by Editor-in-Chief Ahmet Selim Dalkılıç

simulations during nighttime operation. MATLAB code was used for implementation. When compared with existing experimental data, the prediction of the average fin temperature was found to be inaccurate by 5.16% over the collector's full operating duration, including both overnight and daytime operation [1]. Energy from solar collectors should be used as a sustainable power source because of increasing levels of ozone-depleting substances. Field testing and CFD simulations were used to demonstrate the performance of the heat-pipe evacuated-tube solar collector (HPETC) [2]. Nano-liquids enhanced heat absorption in ETSCs, and the Cu-water nano-liquid demonstrated the greatest warm recovery. Thus, to enhance the rate of heat transfer, ETSC's warm exhibition needs to be enhanced [3]. Simulation expression programming was used to model the ETSC for different volumes of thermal storage tanks and different levels of solar radiation intensity, which found a maximum energy efficiency of 72% [4]. Two different types of low-temperature solar collectors, FPC and ETC, flat plate solar collectors and water-in-glass evacuated tube solar collectors, were examined with respect to thermo-hydraulic performance and entropy generation rate. To determine the difference in performance between the two solar collectors, the absorber areas of both were assumed equal. In the context of the Mexican state of Guanajuato, the first analysis was carried out of the operation of the solar collectors with a view to the variation of volumetric flow rates and the values of solar radiation [5]. A new plan for an even tank to store hot water is proposed. CFD reproductions revealed that when the amount of intensity pipes increased, the normal temperature of the level tank also increased [6]. A study analyzed 25 parameters and 259 distinct collector geometries, revealing that tube diameter, absorber area, and mass flow rate significantly influence thermal performance. The optimal geometry had a minimum absorber area of 2.49 m^2, which is significantly less than that of the commercial design. The study's findings could be useful for designing low-temperature, water-in-glass, evacuated tube solar collector networks for heating water in various applications [7]. Previous research did not address the effect of using simulation programs to reduce the cost of manufacturing tests and to obtain faster and more accurate results.

Bouhal et al. [8] reconstructed the increase in intensity in two segments of solar radiation of the evacuated tube solar collector, namely the flat evacuated tank and the flow pipe. Parametric studies of the shape of the intensity lines showed that rectangular pipes were optimal. Water information and exit should be arranged at the base and top of the course pipe as suggested [8]. The efficiency of the solar radiation rises when the flow rate of the liquid increases, and the best results are provided by the filled-type emptied tube with graphite [9]. In this case, CFD was employed in the evaluation of the water temperature at the outlet of the solar collector, where the BA model was seen to be more appropriate than the VPT model [10]. Some powerful cycles have been established to attain the conduct of an evacuated tube solar collector without experimental tests, and CFD has been applied to pay more attention to the heat transfer problems [11]. Previous research did not investigate adding an external enclosure to increase thermal insulation and thereby improve thermal efficiency by raising the temperature of the fluid inside the solar evacuated tube.

The energy, momentum, and temperature (CFD) frontier equations can be used to evaluate the pressure losses resulting from fluid motion in the fins used [12]. Some of the research was aimed at the investigation of solar water heating by the use of evacuated tube solar collectors with CFD software [13]. Little improvements can be made to evacuated-tube solar collectors; however, these improvements may not be cost-effective [14]. Shah and Furbo [15] investigated two vacuum tube designs to prevent solar collector overheating. The study employed numerical solar-thermal modeling and a fourth-order approximation of the efficiency function. Two modified vacuum tubes were studied: one with increased infrared emissivity and the other with an increased convective heat-transfer coefficient. The heat-loss processes were simulated. The performance of these collectors at low temperatures was examined, and the first modified design reduced the collectors' performance by up to 26%. The second design increased infrared heat losses but otherwise had no effect. The researchers found that increasing the number of vacuum tubes could improve performance on overcast days. A solar collector based on a 200-liter water tank could provide hot water for 200 kg/s at 318 K even on overcast days [16]. The research relied on a microfluidizer processor to produce a nanofluid in a two-step SiO_2/water system. In experiments, the thermal conductivity and transmission capability of the nanofluid with mass fractions of 1%, 3%, and 5% have been examined. We simulated heat transfer numerically to determine how the working fluid could have influenced the system. The tests showed that for the SiO_2/water nanofluid, the heat-transfer properties were better than those of water and increased with mass fraction. Another significant factor was the timing of nanofluid placement. According to the study results, longer placement time and increased agglomeration lead to homogenization and increased nanofluid utilization, resulting in more severe deterioration.

Yan et al. [17] center their study on vaccine tube collector BIST systems and how they will handle the environmental effects. The experimental apparatus was built and tested at the University of Corsica, France, and a life-cycle analysis was carried out. In this work, we determined that the energy-payback durations for flat-based integrated solar thermal/BIST and vacuum tube/BIST systems are 1.8 and 0.5 years, respectively. Recycling reduces these durations to 0.5 and 0.1 years. The results of the study were evaluated based on the literature and concluded that the replacement of the vacuum tube/BIST system with a flat plate/BIST system produced a more pronounced effect on the [18]. A linear Fresnel reflector, equipped with an evacuated tube and a CPC secondary reflector was included in the overall study of HTF (HTF = heat transfer fluid). A three-dimensional reconstruction of the vascular system was performed using Monte Carlo Ray Tracing(MCRT), and the results were compared with the actual flow through the system for each case. A 3D optical model was developed to demonstrate the relationships between parabolic and cylindrical mirrors and the influences of temporal changes, varying locations, slope inaccuracies, etc. To ascertain thermal performance, the MCRT and the Finite Volume Method (FVM) were used as the key coupling methods. Given such optical efficiency at normal incidence for mirrors achieving a high sun concentration level, the optimized mirrors came as close as possible to parabolic mirrors, reaching a range of 55.2% to 34.8% for the yearly mean optical efficiency. The radiation temperature trace of the solar collector exhibited some irregularities as solar radiation varied, resulting in solar collector efficiencies exceeding 46.0% under different conditions. This approach can be based on the fact that solar salt can act as the HTF in a Fresnel system environment [19]. Previous researchers rarely quantified the size of the enclosure; instead, they established the major components of the thermal insulation.

Sultana et al. [20] investigated a modified SPETC for utilizing solar heat transmission efficiency and reducing heat loss from a single pass. The SPETC contains six expansion joints and a double-enclosed tube filled with a single-glass material with a selective absorption coating. A symmetrical compound parabolic concentrator (CPC) was constructed using high-reflectivity 3M mirror sheets. This three-dimensional CFD model was built and validated against experimental data to describe the thermal behavior of the SPETC with the CPC-structure telescope reflector. Testing was conducted at a temperature difference of 59.6 K and a volumetric flow rate of 0.0077 m^3/s, which suggests that the machine can achieve a thermal efficiency of 48% daily. The proposed operational volume flow rates of the SPETC, expressed in powers of ten, are between 0.007 and 0.01 $m^3\ s^{-1}$, depending on the HTF (air). It was proposed that the novel SPETC system can be integrated with an adsorption chiller and desiccant wheel to desiccate industrial process heat [19]. Façao and Oliveira [21] proposed low-cost solar thermal MCT (micro-concentrating collector) with LFR (linear frequency reflector) technology for high temperatures reaching 493 K. . MCT focuses on minimizing convective losses and, by utilizing natural convection and radiative heat exchange, achieves total thermal efficiency. A CFD model was developed in ANSYS-CFX to investigate the effect of radiation and convection on absorber temperature. The MCT's greatest feature is that it achieves a higher thermal efficiency at high temperatures than other types, such as flat-plate or evacuated-tube solar collectors. MCT The annual performance for household hot water applications in Australia was computed using TRNSYS [21]. The conic structure of a trapezoidal collector in a linear Fresnel solar collector is modeled and optimized using ray-tracing and CFD simulations. The ray-trace simulation has been acknowledged as potentially applicable to the number of absorber tubes and the slope of the lateral wall. CFD analysis of injection molding determines the optimal insulation contour and thickness using the cavity as a reference. For this simulation, a power-law fit was chosen, which is based on the area of the main mirror. With the help of experiments, the coefficient of temperature heat transfer for linear prototypes of Fresnel is compared to correlation data by Larkin [22].

The literature review discusses various approaches used to boost the performance of empty-space solar collectors, such as the application of nanofluids, exposure to a magnetic field, and the addition of vanes or fins. While they are effective at transferring heat, these methods usually employ expensive that hinder everyday application. Using CFD, FVM, and MCRT, engineers can now build and test their designs on computers, eliminating sole reliance on experimental equipment. Experts have demonstrated that how a collector captures energy depends on its geometry, tube width, and flow rates. In addition, experts have found that environmental variables such as ambient temperature, the sun's position, and seasonal variation affect the way the system functions. Nevertheless, many people do not consider external enclosures an effective means of passively reducing heat loss. Therefore, this study proposes a simple, economical enclosure that significantly improves heat transfer, providing a practical solution for solar thermal systems.

The research of Roshani et al. (2024) [23] focused on natural convection within triangular cavities that contained obstructions of inverted triangle shape along with square and rhombus designs made from nanofluids. The researchers discovered that rising Rayleigh numbers intensify liquid velocities by producing vortices, while sinusoidal temperature conditions enhance heat transfer by inducing flow patterns. The authors demonstrated how obstacle shape and thermal conditions work synergistically to enhance heat transfer. Jalili et al. (2025) [24] performed thorough numerical research that examined heat transfer phenomena in porous media with different-sized square vanes positioned at cavity corners. According to their research, the Nusselt number, entropy generation, and thermal performance were substantially influenced by geometrical adjustments; thermal performance improved significantly when the Hartmann and Darcy numbers increased under an applied magnetic field. The research conducted by Bahmani et al. (2024) [25] analyzed both regular and irregular vanes embedded inside pipe-shaped porous cavities. Research conducted by Bahmani et al. (2024) [25] demonstrated that using irregular vane shapes produced greater changes in stream function properties and heat transfer performance while granting a near 90% improvement to Nusselt number measurements compared to regular vane designs. A wavy square porous cavity was examined regarding its reaction to partial magnetic fields by Mirzaei et al. (2024) [26]. The researchers demonstrated that suppression of heat transfer by magnetic fields decreased as additional wall waves were added to the system, while the field area coverage was also varied. Jalili et al. (2024) [27] produced significant advancements by studying double-diffusive natural convection inside a porous-fluid cavity with slope orientation. Heat transfer (Nusselt number) decreases as porous layer thickness increases until a point is reached at which the Nusselt number begins to increase again. Research has shown that the slope angle of the cavity plays an important role in thermos-solutal convection, as increased Rayleigh and Darcy numbers produce sustained enhancements in heat transfer.

The rationale behind choosing these particular methods for their study, as well as how they ensure consistency and reliability across different simulation techniques, is that MATLAB is a popular platform for numerical simulations and data analysis, particularly for studying solar thermal systems. It offers capabilities for heat transfer, fluid dynamics, and radiation modeling, which are crucial for studying solar evacuated-tube receivers. CFD (computational fluid dynamics) is used to analyze fluid flow patterns, heat transfer, and turbulence within receiver tubes and enclosures. MCRT (Monte Carlo Ray Tracing) is used for modeling radiative heat transfer in complex geometries, allowing for accurate estimation of radiative heat fluxes and temperature distributions. FVM (Finite Volume Method) is used to solve the partial differential equations governing fluid flow and heat transfer, making it suitable for studying the thermal performance of solar receivers and enclosures. To ensure consistency and reliability, models are validated against experimental data or analytical solutions, and sensitivity analyses and convergence studies are conducted to assess the impact of parameters. This approach enhances the credibility of findings in solar thermal energy research.

In our approach, originality lies in obtaining maximal thermal energy in the evacuated tube collector and achieving the highest temperature for the pipes of the evacuated tube solar collectors. It will be made possible by implementing tubular collector with a sun-reflective wall painted to achieve high thermal gains and an internal dark screen to prevent radiation from escaping. To increase the efficiency and performance of solar evacuated tubes, the project will develop and sequentially implement the enclosure system. The sunlight-collection capability of these devices is highly dependent on environmental variables, such as temperature, wind, and humidity. The performance of these devices, therefore, may be significantly affected by these factors. The objectives of the project comprise safeguarding the pipes from the elements, taking advantage of atmospheric conditions, inspecting the effectiveness of the enclosure, and assessing how well it improves efficiency. This work aims to design and construct a protected microenvironment, develop a temperature control system with built-in mechanisms to limit the impact of wind and humidity, and conduct research and data analyses to evaluate whether the mitigation of a barrier results in a further increase in crop yield. The study does not employ vacuum tubes as its primary target; instead, it focuses on the obstruction of the surrounding airflow.

Current techniques for heat transfer enhancement in thermal systems involve making internal modifications by reshaping fluid flow patterns or adding obstructions within cavities , to increase the Nusselt number and improve thermal gradients.

Research on thermal insulation techniques that prevent environmental heat loss from cavities remains insufficient, despite their ability to preserve fluid behavior. Research into external enclosures for heat retention around evacuated tube collectors remains understudied, and past findings do not provide quantitative measurements of enclosure shapes, solar-angle orientations, or seasonal performance.

Knowledge Gap: Although many researchers have investigated internal modifications that improve the performance of solar evacuated-tube collectors—namely through nanofluids, magnetic fields, or optimized geometries—there is scant literature on the contribution of external enclosures or passive heat holders. Moreover, the available literature has not fully explored the effects of enclosure gap dimensions and azimuth angle on thermal performance across seasons. Moreover, the majority of optimization techniques use expensive, actively powered systems or complex materials that are not feasible for intensive integration into residential or other off-grid systems due to integration costs.

These gaps have been addressed in this research by providing a novel, simple, and cost-effective solution: an external enclosure system that reduces heat losses to the environment, improves thermal efficiency, and does not require complex active components or expensive materials. This study explores influence of different gap thicknesses(10 cm, 20 cm, and 30 cm)and azimuth angles(0 and 40 degrees)on the thermal characteristics of solar evacuated tube collectors, thus giving us a comprehensive view of how the environment will affect these collectors. Furthermore, the research examines the possibility of using external enclosures as a reliable yet low-cost alternative for improving performance under summer and winter conditions, and thereby addresses the absence of information regarding seasonal performance under changed conditions in earlier literature.

Novelty/originality: Through extensive numerical calculations, this project establishes for the first time that external enclosures enhance the efficiency of evacuated tube collectors by effectively reducing environmental heat losses. The passive improvement approach enables design enhancements applicable to for any climate zone and installation space through the simple implementation of existing technologies. The paper proposes an innovative method for solar thermal power that focuses on the non-energetic aspects of enclosures. It is also cost-effective and energy-efficient, the required materials, such as glass and coated steel, are simple. They have not widely used this type of design with evacuated tube collectors , and the paper provides an in-depth numerical study conducted using the COMSOL Multiphysics simulation program. Without the use of advanced tracking facilities and expensive materials, the enclosure system can achieve a high thermal efficiency (94.29 per cent) and an internal temperature of 328 K. The literature contains a limited number of prior studies, since many have not focused on how enclosure gap size, solar azimuth angle, and seasonal conditions relate; this study addresses that question. This system is simple, affordable, and can therefore be used in small residential or off-grid installations.

2. Methodology

Because of changing patterns in solar radiation, research is being conducted to study renewable energy resources. An analytical model of solar radiation at the ground surface is applied to study changes in received solar radiation as a function of the solar collector angle. The 3D model was developed using mathematical equations and Cartesian coordinates (x, y, z). They are then linked to perform the simulation in COMSOL 5.6 using the provided equations and mathematical formulations. The COMSOL program is run by selecting a simulation model. This model includes solar radiation and heat transfer between the fluid and the solid. The solar radiation area is selected, the latitude and longitude lines for the area for which radiation will be calculated are added, and then the date and time are entered. After this stage, the domain to be used is defined, its dimensions are given below, and the materials, including water and clay, for both the solar complex and its dimensions are determined. First, the heat transfer areas are fixed; then a mesh suitable for the simulation is generated; finally, the simulation time is determined as 12 hours, from five in the morning to five in the evening.

The proper choice of material for the enclosure is essential for enhancing efficacy, since it greatly reduces heat loss to the surroundings. It has a glass front because glass allows a lot of sunlight in and does not readily let heat escape. Polycarbonate might be superior with respect to impact resistance, but its performance degrades when exposed to sunlight. Usually, the back wall is constructed from coated steel or other materials painted black to absorb more solar energy, but this setup could lead to conductive heat loss if the space is not properly insulated. The choice of materials affects both the cost and efficiency of a building because glass costs less than polycarbonate, whereas steel ensures structural integrity but requires protection against corrosion. All materials must be resistant to changes in temperature and environmental factors. Describing the exact materials used and their optical, thermal, and cost characteristics can help us understand how the enclosure contributes to the system's long-term efficiency and reliability.

To ensure the proposed method is useful, its costs and benefits must be examined to determine how it measures up against reflectors. Passive insulation is used in the enclosure system, which consists of walls of glass and steel; the structure is relatively simple. It raised the temperature by 7 K and provided a thermal efficiency of up to 94.29%, while requiring no energy input or moving components. On the other hand, reflectors achieve better results but entail higher upfront and maintenance costs and require additional energy to operate. Because it is very energy-efficient, long-lasting, and affordable, the enclosure method is widely chosen for situations involving small installations or remote areas. Including this analysis would strengthen the study's case for adopting the rules and would demonstrate the issues readers might encounter when applying these in real cases.

Unlike before, the researchers used passive skirting around the solar evacuated tubes and did not use nanofluids, make internal modifications to the tubes, or employ active sun-tracking methods. Rather than modifying internal water flows or introducing more expensive materials, this paper examines the use of common materials (glass) to insulate the external environment and assesses their impact through detailed year-round simulations. The simulation tests the effect of three types of enclosure gaps (10 cm, 20 cm, and 30 cm) and compares their performance at two azimuth angles (0° and 40°). With this method, solar thermal collectors become more efficient and economical, benefiting off-grid and residential users who prioritize simplicity and cost efficiency.

2.1. Governing equations

The COMSOL Multiphysics platform is applied to model fluid dynamics, thermal phenomena, and radiative effects in the system by solving the governing equations with high fidelity. These are coupled multiphysics that model complex interactions among heating and cooling processes and the flow of a heat-transfer fluid. Mesh refinement and mesh-independence studies are performed to ensure simulation fidelity by minimizing numerical errors. The experiment is also validated using past experimental results to verify the model's thermal performance. The strength of the model has enabled one to gain reliable insights into thermal patterns and temperature distributions across various enclosure gap frequencies, azimuthal angles, and seasonal conditions. Major transformations involve application, fidelity to detail, and simplification of mathematical technicalities.

The surface-to-surface view factor quantifies the energy incident on one surface from another. This view factor is the fraction of the energy leaving the first surface that is received by the second surface. In 3D, the calculation of a view factor involves clusters of faces, whereas in 2D it is based on mesh faces. The incident energy flux can be expressed in terms of the energy flux leaving all other surfaces as follows:

$$A_k q_{in,k} = \sum_{j=1}^{N} A_j q_{out,j} F_{jk} \tag{1}$$

A_k is surface area of k and F_{jk} is view factor between surface j and surface k. For N surfaces, using the view factor reciprocity relationship:

$$A_j F_{jk} = A_k F_{kj} \quad \text{for } j = 1,2,3, \ldots N \tag{2}$$

so that

$$q_{in,k} = \sum_{j=1}^{N} F_{kj} q_{out,j} \tag{3}$$

Therefore,

$$q_{out,k} = \varepsilon_k \sigma T_k^4 + \rho_k \sum_{j=1}^{N} F_{kj} q_{out,j} \tag{4}$$

which can be written as

$$J_k = E_k + \rho_k \sum_{j=1}^{N} F_{kj} J_j \tag{5}$$

J_k: energy that is given off (or radiosity) of surface k, and E_k: emissive power of surface k. Which represents N equations, and can be recast into:

$$KJ = EJE \tag{6}$$

K : an $N \times N$ matrix, J : vector of radiosity, and E is vector of emissive power. The view factor between two finite surfaces i and j:

$$F_{ij} = \frac{1}{A_i} \int_{A_i} \int_{A_j} \frac{\cos\theta_i \cos\theta_j}{\pi r^2} \delta_{ij} \, dA_i \, dA_j \tag{7}$$

where δ_{ij} is determined by the visibility of dA_j to $dA_i \cdot \delta_{ij} = 1$ if dA_j is visible to dA_i and 0 otherwise.

The View Factor F_{ij} represents the fraction of radiation leaving surface i that strikes surface j. It depends on the geometry and orientation of the surfaces. The governing equations used to calculate view factors describe geometric relationships and are typically derived from the surfaces' configuration. The Stefan-Boltzmann law describes the radiation emitted by a surface due to its temperature. It is given by the equation:

$$Q = \varepsilon \times \sigma \times A \times T^4 \tag{8}$$

Q: heat transfer rate of radiation, ε: emissivity of the surface, σ: constant of Stefan-Boltzmann, A: surface area, and T: absolute temperature of surface.

Radiative two surfaces is expressed as the net radiation exchange, which is the product of the view factors and the Stefan-Boltzmann constant. It can be expressed as:

$$Q_{net} = F_{ij}(\varepsilon_i \times \sigma \times A_i \times T_i^4 - \varepsilon_j \times \sigma \times A_j \times T_j^4) \tag{9}$$

Ai and A_i: surface areas, Q_{net}: rate of net heat transfer, F_{ij}: view factor from surface i to surface j, i and j: surfaces' emissivities, and Ti and Tj: absolute temperatures of respective surfaces'.

The numerical simulation of the solar evacuated-tube system with an enclosure was conducted using COMSOL Multiphysics, incorporating fundamental Computational Fluid Dynamics(CFD)equations to model heat and fluid transport. These equations include:

1. Continuity Equation(Mass Conservation):

$$\nabla \cdot \vec{u} = 0 \tag{10}$$

This equation ensures the conservation of mass for an incompressible fluid, where $\vec{u}$ is the velocity vector.

2. Momentum Equation(Navier-Stokes Equations):

$$\rho\left(\frac{\partial \vec{u}}{\partial t} + \vec{u} \cdot \nabla \vec{u}\right) - -\nabla p + \mu \nabla^2 \vec{u} + \vec{F}$$

This equation governs the motion of the fluid, where ρ is fluid density, p is pressure, μ is dynamic viscosity, and $\vec{F}$ represents body forces such as gravity.

3. Energy Equation(Thermal Energy Conservation):

$$\rho c_p\left(\frac{\partial T}{\partial t} + \vec{u} \cdot \nabla T\right) = \nabla \cdot (k \nabla T) + Q \tag{12}$$

This equation accounts for heat transfer due to conduction, convection, and internal heat generation, where T is temperature, c_p is specific heat capacity, k is thermal conductivity, and Q represents volumetric heat sources (e.g., solar radiation absorption).

4. Radiative Heat Transfer(Surface-to-Surface Radiation using View Factor method):

$$q_{Tad} = \sigma\varepsilon\,(T_s^4 - T_{sur}^4)\,F_{ij} \tag{13}$$

Where σ is the Stefan-Boltzmann constant, ε is emissivity, T_s is surface temperature, T_{sur} is surrounding temperature, and F_{ij} is the view factor between surfaces.

These governing equations were solved using the Finite Volume Method (FVM) under steady and transient conditions to evaluate heat distribution within the enclosure and the evacuated tubes. The simulation incorporated solar irradiation, natural convection, and thermal radiation to accurately represent the physical phenomena. Validation through mesh-independence testing and comparison with previous research confirmed the robustness of the numerical outcomes.

To clarify the thermal performance analysis, thermal efficiency (η_{th}) was computed using:

$$\eta_{th} = \frac{\dot{m} \cdot C_p \cdot (T_{out} - T_{in})}{A_c \cdot G_t} \tag{14}$$

In the optimized case (10 cm gap, 0° azimuth, summer at 1:00 p.m.), the following values were used:

Mass flow rate, $\dot{m} = 0.0341 kg/s$

$T_{in} = 305K, T_{out} = 314.5K$

Specific heat of water, $C_p = 4186 J/kg \cdot K$

Collector area, $A_c = 1.8 m^2$

Solar irradiance $G_t = 800 W/m^2$

Then:

$$Q_{useful} = 0.0341 \cdot 4186 \cdot 9.5 = 1357.78W$$
$$\eta_{th} = \frac{1357.78}{1.8 \cdot 800} = \frac{1357.78}{1440} = 0.9429 \approx 94.29\%$$

2.2. Mesh generation

Table 1 shows that the solar collector was designed based on the dimensions of the existing factory. Allowing unstructured 3D grids as an option is highly recommended in such cases, since they are well suited to complex geometries. A 3D model geometry mesh was created in COMSOL. This work was carried out using 279224 cells in total; detailed images of these cells are presented in Figure 1.

Table 1. Specifications of evacuated tube [28]

Inner Tank	Imported SUS304-2B stainless-steel, 0.5 mm^2				
Outer Tank	Coated steel: 0.4 mm^3				
Vacuum Tube	Solar vacuum tube D58-L1800 mm				
Frame	Coated steel: 1.2-1.5 mm				
Workmanship	Employ automatic argon arc welding method; have better pressure performance; have better antisepsis performance in the welding seam; no leakage for a long time. Applying the automatic machinery foaming technique, superinsulation capacity				
Water tank	Quantity	tube Diameter	Length	Tank's capacity	Net weight
460 mm	30	58 mm	1.8 m	300 L	123.2 kg.s

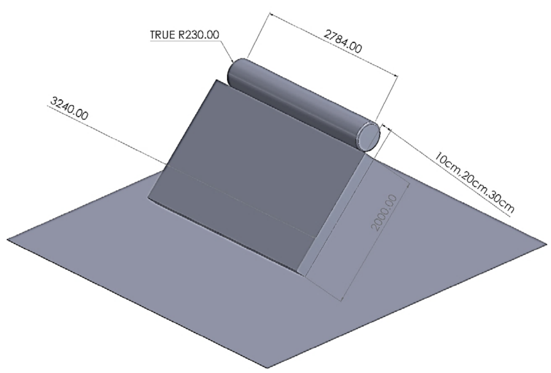

(a)

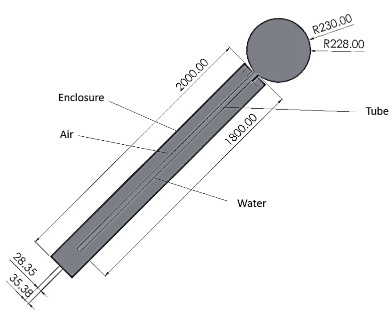

(b)

Figure 1. Geometry of system with dimensions, **(a)** the domain ans **(b)** the side view

A container with a glass front and an absorptive back wall was built to enclose the pipes and contain an air gap to increase absorption of heat from solar radiation; three gap dimensions were used: 10 cm, 20 cm, and 30 cm. The enclosure measured 3240 mm in length and 2000 mm in width.

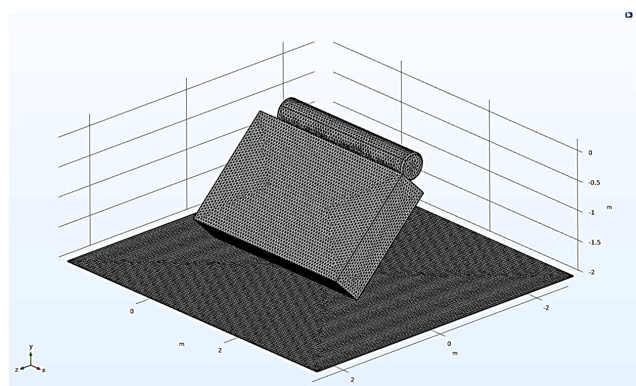

Figure 2. Mesh generated

To obtain more precise data, the mesh size should be adjusted to allow tracking of the output as the number of elements increases. Mixture stability is the final point reached when the mesh size is 0.001 m. Therefore, the procedure concludes and is shown in Figure 2 and Table 2.

Table 2. Mesh independency

Case	Element	Max Average volume temperature (°C)
1	120345	320.5
2	193644	315.8
3	241545	314.6
4	279224	314.5

2.3. Conditions of boundary

Reflective mirrors, with a reflectance of 0.8, were used behind the solar array to reflect more solar radiation than was incident on them . The container has a front glass panel to collect the rays and confine them within the container, as illustrated in the figure below. To perform the following calculations to estimate the amount of incident solar radiation with a high degree of accuracy, the coordinates of the target location (Baghdad) were identified the year, month, day, and hour. Two time points were taken: the 7th month of the year (July), which represents the summer, and the 2nd month of the year (February), which represents the winter (1st month). The properties of the solar heater material and the evacuated tube are then determined, and the altitude angle is set from 0 to 40 degrees at one-hour intervals from 5 a.m. to 5 p.m. Thermal details, such as the average air volume temperature and the amount of solar radiation, are added automatically by the simulation program when the user specifies the day, month, year, longitude, and latitude, as shown in Figure 3.

The following are the thermal and environmental input parameters:

1. Material Thermal Properties

Table 3 shows the thermal properties of the material.

Table 3. Material thermal properties

Component	Material	Thermal Conductivity (W/m·K)	Emissivity	Specific Heat Capacity (J/kg·K)	Thickness (mm)
Front Cover	Glass	~1.0	~0.88	~750	4
Back Wall	Coated Steel (black)	~50	~0.9	~500	1.5
Insulation Layer	Air gap	0.026 (natural convection)	–	–	100–300
Vacuum Tube	Borosilicate Glass	~1.1	~0.85	~800	~2

Table 4. Enhanced material selection justification

Property	Glass (Low-iron)	Polycarbonate	Coated Steel (Black Painted)
Thermal Conductivity	~1.0 W/m·K	~0.19 W/m·K	~50 W/m·K
Solar Transmittance	85–91%	88–92%	~5–10% (absorptive, opaque)
Emissivity	0.88	0.85–0.90	0.90 (black painted)
Durability (UV Resistance)	High	Low (degrades with UV)	High
Cost (USD/m²)	~$30–40	~$45–60	~$15–25
Notes	High solar transmission, rigid, scratch-resistant	Lightweight, flexible but less durable	High thermal absorption, structure support

Glass (particularly low-iron or tempered glass) has high ultraviolet resistance and excellent long-term optical stability; in contrast, polycarbonate fades and becomes yellow through sun exposure. However, its transmittance would decrease by 46% within six months due to dust and debris unless it is kept clean, especially in arid environments. In remote installations, passive, low-maintenance materials such as glass and coated steel are advantageous: both can be easily rinsed, and coated steel is resistant to corrosion. Other features that reduce maintenance are tilted panels, removable glass parts, and dust-resistant coatings. Structurally, tempered glass can endure wind loads of up to 2500 Pa when supported by a suitable frame, and coated steel will add rigidity; therefore, an enclosure designed to an appropriate standard, such as ASCE 7-22, can resist wind loads.

Some aspects of optimization, mainly concerning enclosure design (e.g., air gap and azimuth angle), have already been factored into the study, but the researchers indicate that the results would be improved by a series of tests varying other parameters, e.g., alternative materials or the inclusion of phase change materials (PCMs). Nevertheless, the application of a more generic design prescription, founded on parametric optimization, would enable the scaling and replication of a rudimentary design syntax that could be implemented across a range of geographical and climatic contexts. The parametric optimization used in the study would enable identification of the most informative variables (e.g., materials, solar irradiance, environmental conditions) and would also enable the development of a systematic process for designing variables with minimal cost but optimal efficiency. This may result in a universal guideline for designing solar evacuated-tube collectors that are not only efficient but also cost-effective in meeting the specific demands of various environments. The availability of simulation tools (e.g., COMSOL or CFD) for evaluating different configurations across a range of conditions is an advantage of the study.

2. Boundary Condition Assumptions

Ambient Temperature ($T_{ambient}$):

- Summer (July) temperatures varied between 305–313 K(32–40 °C),based on Baghdad climate data.
- Winter (February): Varied between 285–290 K(12–17 °C).
- Variation applied as a time-dependent boundary condition (hourly input).

Solar Irradiance:

- Simulated from 5:00 a.m. to 5:00 p.m.
- Used hourly direct normal irradiance (DNI) and diffuse horizontal irradiance (DHI) values from typical meteorological year (TMY) data for Baghdad.

Convective Heat Transfer Coefficients (h):

- External natural convection and internal natural convection coefficients are established based on conventional literature values. In case of external natural convection, 5-10 W/m^{2}K is selected, which follows natural air convection at the external air surface. In the case of internal natural convection, 2-5 W/m^{2}K is applied which is within the normal range of a gap through which the natural convection is likely to contribute to heat transfer.

- Wind Speed: 1.5 m/s typical wind for July in Baghdad.
- Reflectivity of Back Mirror: 0.8.

In systems where solar energy is used to heat water, the azimuth angle determines the collector's direction relative to true south when located in the Northern Hemisphere and has a significant influence on the exposure to and power received from solar radiation. A 0° azimuth usually indicates the optimal orientation for facing the sun at solar noon to receive more solar energy. The 40° angle is realistic because factors such as roof orientation, building placement, or shading may necessitate adjustments during installation.

The characterization of solar irradiance in this study is based on meteorological data, namely the typical meteorological year (TMY) data for Baghdad in order to accurately model environmental situations with respect to their effects on the behavior of solar collectors. The data record variations in irradiance caused by time of day, season, and cloud cover. Data from the summer (July) and winter (February) months are chosen to simulate the system performance under the extreme seasonal conditions, as occurs during high and low solar intensities. The solar angle and the path taken by the sun throughout the day are also accurately taken into account using the latitude and longitude of Baghdad; hence, the model can comprehensively represent solar radiation on the evacuated tube collector at any time of day in summer and winter.

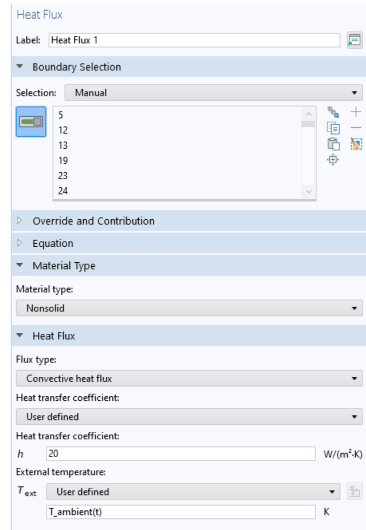

(a)

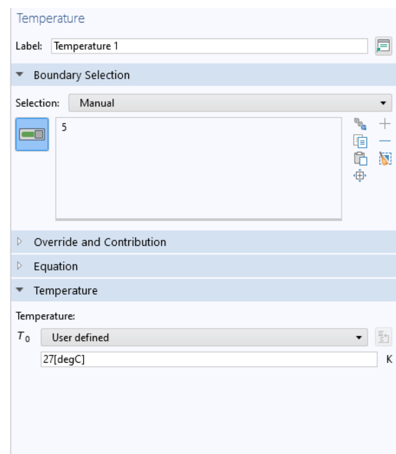

(b)

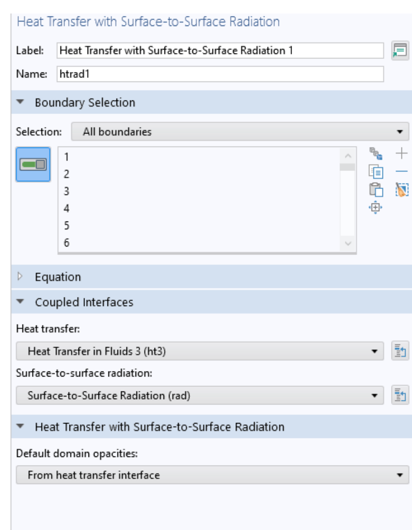

(c)

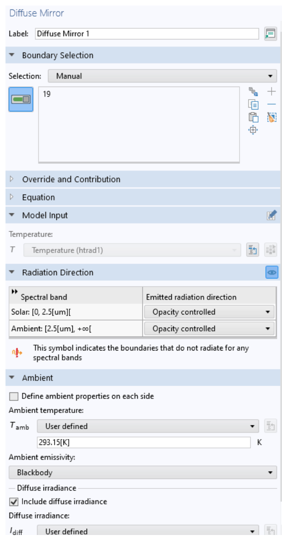

(d)

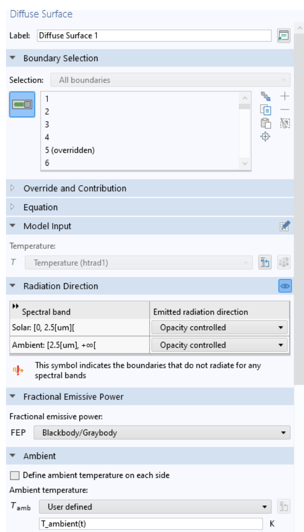

(e)

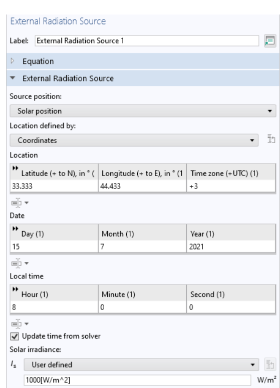

(f)

Figure 3. Program selections, **(a)** heat flux, **(b)** temperature, **(c)** heat transfer with surface-to-surface radiation, **(d)** diffuse mirror, **(e)** diffuse surface, **(f)** external radiation source.

This study examined the thermal characteristics of solar evacuated-tube collectors by implementing an external heat-retaining enclosure designed to reduce heat loss. A numerical simulation of heat transfer was implemented in the solution method using the COMSOL Multiphysics platform to model the three-dimensional enclosure system. The simulation included air gaps of three different sizes (10 cm, 20 cm, and 30 cm) to determine their impact on temperature distribution within the enclosure system.

Solar radiation heat flux, combined with natural convection and thermal conduction, enabled the simulation to analyze the enclosure materials and air gap. The simulation used solar irradiation between 5 am and 5 pm,two azimuth angles (0° and 40°), and temperature variations representing summer and winter. In the simulation, reflective surfaces were assigned a reflectivity coefficient of 0.8, representing the installed mirrors behind the tubes. The heat transfer model that used the surface-to-surface view-factor method to model radiation heat transfer between enclosure walls and evacuated-tube surfaces solved the steady-state and transient energy equations.

A mesh-independence study was conducted to verify numerical precision; convergence was reached at 279,224 elements. The computational model generated simulated data on the internal enclosure temperatures, the average chamber temperature of the evacuated tube, and thermal performance over time. Results were consistent with previous experimental and numerical studies, which indicated that enclosing tubes helped increase maximum average temperatures from 321 K to 328 K. The solution method presents a validated physical approach for determining changes in the thermal behavior of solar evacuated tube collectors subjected to enclosure variations under operational conditions.

3. Result and discussion

The results will be discussed with regard to the placement of the container and to the details of its dimensions. Differences between seasons (environmental conditions) will also be discussed, as will differences in the orientation angle of the solar collector.

Average volume temperature: The temperature averaged throughout the complete solar evacuated tube collector system (or the collector tube in the case of collector tube-focused systems). It is a fixed view of the mean distribution of heat in the system at a specific time or under certain environmental conditions. The value of this metric is usually determined by measuring the average temperature at different points in the system that collects temperature values.

Internal temperature refers to the temperature inside a collector tube or in the surrounding enclosure of an evacuated tube. This term usually refers to the temperature of the fluid or air within the system, which is warmed by solar radiation captured by the collector.

The simulation outcomes presented in this paper are deterministic, derived from steady-state and transient analyses, and do not include statistical measures such as standard deviations or margins of uncertainty. All reported temperature values and thermal-efficiency results pertain to a single simulation scenario with fixed environmental and geometric settings. Although the study did not fully quantify uncertainties or perform sensitivity analysis, numerical tolerance and convergence were achieved through a mesh-independence test, which is reported in Table 2. In this way, confidence in the reliability of the simulation results is increased; ideally, future work can employ uncertainty quantification to more effectively sample variability in environmental inputs and material properties.

3.1. Effect of enclosure volume on temperature

The average temperature of the volume inside evacuated tubes depends mainly on the surroundings; the tubes prevent heat loss and maintain a continuous flow to absorb solar thermal energy. Waterproofing the bulk of the compartment makes it practicable to insulate the tube from the average volume temperature using a volume enclosure. Although the surrounding environment must be cooler than the interior of the tube, this lining is an effective insulator that helps maintain higher average internal temperatures. This increase in seawater salinity significantly influences the practicality of solar thermal systems by preventing collected heat from dissipating quickly into the environment. The vacuum tube would dissipate energy more rapidly through these three mechanisms (conduction, convection, and radiation), does not increase the radiating space. The enclosure acts as a barrier that hinders the above-mentioned modes of average-volume temperature transfer within the tube and thus remains at a constant level. Retaining heat during low-radiation periods is crucial for stable performance. Conversely, the high-vacuum enclosure can limit heat from solar radiation that could otherwise overheat the tube. The well-insulated vessel of the inflatable enclosure prevents a large rise in average volume temperature from destroying the sensitive internal components or causing losses of energy due to heat dispersion outside the vessel. To address specific cooling applications, the designer and design engineer can carefully size the enclosure. As an example, they may select materials and thicknesses that function not only to meet the necessary operating average volume temperature range but also to maintain that range and to provide the desired level of insulation. The conversion of solar heat within the glass chambers of evacuated solar tubes enables them to harness solar energy. In conclusion, the volume enclosed by solar evacuated vacuum tubes serves as a thermal barrier that maintains the average operating temperature within the tube at a stable and effective level. To properly capture and store solar energy for use in various solar thermal applications, including the electricity production and space and water heating, a solar thermal system must minimize both excessive heat gain and heat loss.

Figure 4 shows the average volume temperature gradient over time. It is noted that the average volume temperature rises when using the enclosure at 1 p.m., at a distance of 10 cm, reaching 314.5 K. At 20 cm, it reaches 314 K, and at 30 cm, it decreases by two degrees Celsius. In the afternoon, the enclosure retains heat and transfers it to the pipes, which is advantageous for charging the pipes at sunset because of the hot air inside the enclosure.

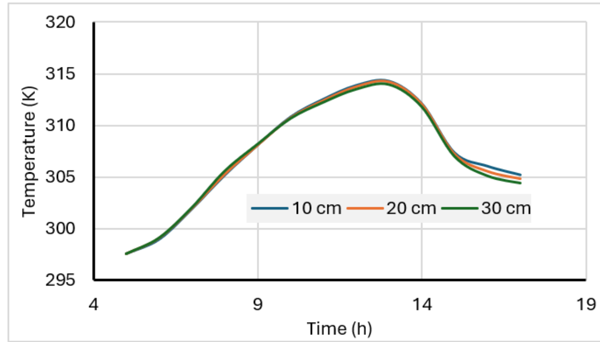

Figure 4. Average volume temperature gradient using enclosure at different space in summer (7th month) and azimuth 0 degree

Figure 5, which shows the effectiveness of using enclosures in thermal confinement of air for improving the reception of heat from incident solar radiation, A size of 10 cm is preferable for thermal confinement at different times. The average volume temperature reached 314.5 K, then gradually decreased in the remaining volumes due to the air's inability to provide sufficient heat during the day.

Figure 5 depicts the average volume temperature in the enclosure at three air-gap sizes (-10 cm, 20 cm, and 30 cm), measured during summer (July) with the solar collector at 0° azimuth. Such charts demonstrate that enclosure spacing helps maintain warmth in a space. The internal temperature of the 10 cm gap reaches as high as 314.5 K, indicating that heat loss is inhibited more effectively (see Figure 5a). At gaps of 20 cm and 30 cm, heat loss is greater, resulting in a lower average volume temperature than at smaller gaps (Figures 5b and 5c). The figures show that heat accumulates more rapidly in smaller spaces with better thermal efficiency. The charts indicate that a 10 cm spacing between the plates yields the highest temperature and the best overall performance of the system.

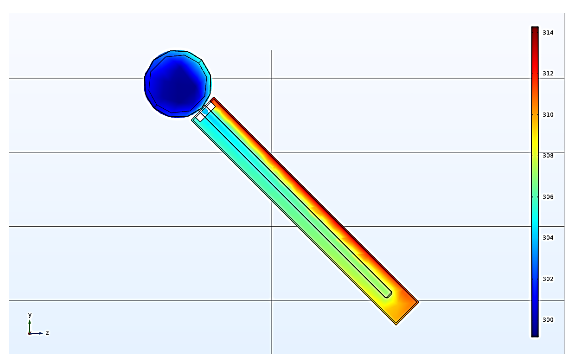

(a)

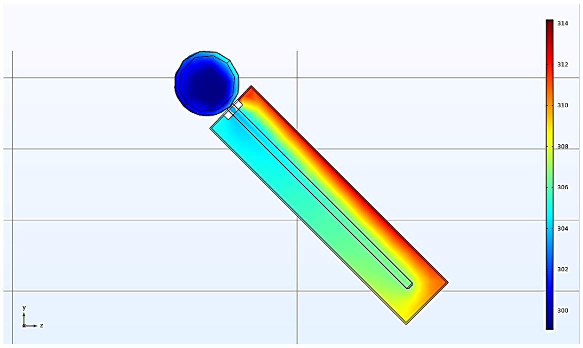

(b)

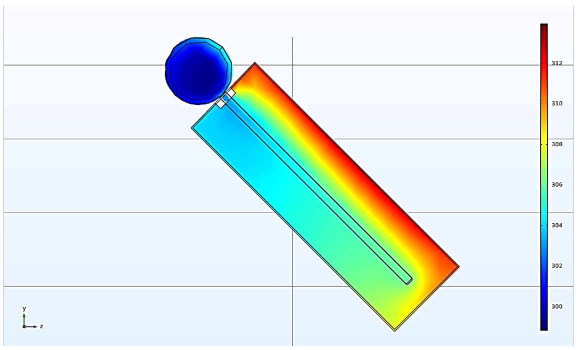

(c)

Figure 5. Average volume contour of temperature using enclosure at different space in summer (7th month) and azimuth 0 degree: **(a)** 10 cm, **(b)** 20 cm and **(c)** 30 cm

3.2. Effect of azimuth degree on temperature

The average temperature inside a solar evacuated tube can be affected by the azimuth angle, which denotes the compass direction toward which the tube is oriented. However, the precise impact varies throughout the day and across the year, depending on a number of variables. The orientation of the vacuum tube with respect to the sun's position in the sky is determined by the azimuth angle. The tube receives the most solar energy when it is aimed directly at the Sun (azimuth angle of 0 degrees). In this research, azimuth angle is the horizontal angle of the solar collector in the Northern Hemisphere measured from geographic due south. Zero azimuth angle at the collector means that the collector faces geographic south, which is generally the optimal orientation at solar noon for maximum irradiation. A positive azimuth angle, such as 40 degrees implies that the collector is turned westward (measured clockwise from south), reflecting more realistic installation conditions in which a perfect orientation may be impossible due to the roof's geometric limitations or nearby obstacles that cause shading. This definition aligns with conventional uses of solar energy and ensures an accurate understanding of diurnal changes in solar exposure. The tube's exposure to direct sunlight decreases as the azimuth angle moves away from 0, which may affect the rate at which the tube collects solar energy. Solar radiation is absorbed by a vacuum tube and transformed into heat energy. The tube will generate more heat when exposed to higher incident solar radiation. The tube will experience its average volumetric temperature rise when the azimuth angle is optimal, which is commonly south-facing in the Northern Hemisphere or north-facing in the Southern Hemisphere. As the sun's position changes throughout the day, the azimuth angle also changes. The tube may heat up more slowly or reach volume-averaged maximum temperatures in the morning and afternoon, when the azimuth angle is lower than when it is oriented directly toward the sun at noon. The impact of the azimuth angle on average volume temperature varies by season. When the sun is lower in the sky during winter (1st month), the azimuth angle becomes more important in regulating the average temperature within the vacuum tube. Even with suboptimal azimuth angles, significant solar radiation may still be received during the summer because the sun is higher in the sky. The effect of azimuth angle on the average volume temperature depends on the location of the solar thermal system. Latitude, regional climate, and the solar path are crucial considerations, since they affect the angle at which the sun traverses the sky. The positioning and tracking (if applicable) of the vacuum tubes, as well as other aspects of the solar thermal system's design, may affect how the azimuth angle influences the average volume temperature. Some systems use tracking technologies to follow the sun's course throughout the day and adjust their angle to maximize exposure to sunlight. In conclusion, the azimuth angle influences the amount of solar radiation that evacuated solar tubes receive, which in turn affects how hot they are internally. The ideal azimuth angle depends on the system's design, season (environmental conditions), and geographic location. Maximizing the performance of solar thermal systems requires achieving the proper azimuth angle. Higher average volume temperatures and heat that is more effectively collected may arise from proper orientation.

Figure 6 shows the effect of the azimuth angle on solar vacuum tubes. The angle of 0 degrees received more solar radiation than the angle of 40 degrees; at 0 degrees the temperature reached 314.5 K, whereas at 40 degrees it was 313 K. It also has the advantage of increasing average volume temperatures during the extended hours of the day.

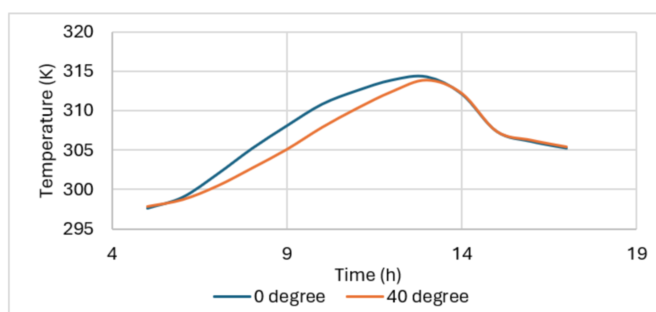

Figure 6. Average volume temperature gradient by using enclosure and 10 cm space in summer at different azimuth degree

Figure 7, which shows the temperature differences between azimuth angles with the enclosure, indicates that the azimuth angle of 0 degrees was thermally superior, reaching 314 K, compared with 40 degrees, which reached 313 K at one o'clock in the afternoon during the summer.

Figure 7 shows the average internal temperature contour inside the container with a 10 cm air gap for the summer season's 7th month at both angles: (a) 0° and (b) 40°. It shows the impact of collector orientation on the absorption and internal distribution of heat. At 0° azimuth, as shown in Figure 7a, the temperature in the enclosure is approximately 314 K, which indicates that it is being heated by direct solar radiation. In contrast, when the Sun is at 40° azimuth (Figure 7b), it delivers less solar energy to the Earth, resulting in a slightly lower temperature of 313 K. It is evident from the comparison that facing the collector due east maximizes solar power intake, so this improves the home's thermal performance during the warmer months.

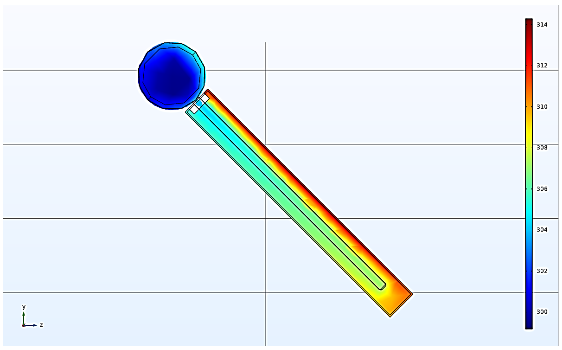

(a)

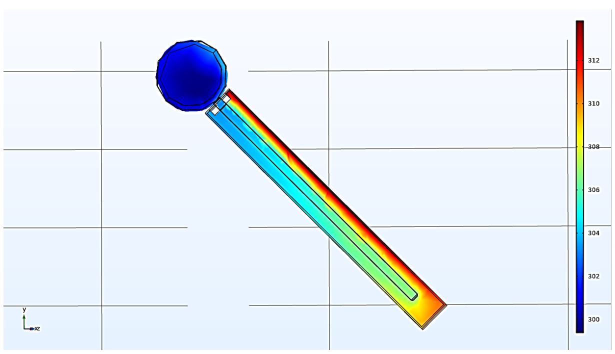

(b)

Figure 7. Average volume temperature contour by using enclosure and 10 cm space in summer at different azimuth degree: **(a)** 0 degree and **(b)** 40 degree

3.3. Effect of environmental conditions on average temperature of tube

The average internal temperature of solar evacuated tubes is significantly influenced by seasonal (environmental conditions), which are mainly driven by variations in solar radiation and other external factors. The exposure of the vacuum tubes to solar radiation is affected by seasonal variations in solar angle and daylength. The tubes typically receive more direct and intense sunlight during the summer, when the sun is higher in the sky and the days are longer. In contrast to winter, when the sun is lower in the sky and the days are shorter, average volume temperatures inside the tubes are warmer. Solar radiation is converted into heat energy in evacuated tubes. The average temperature of the volume inside the tubes can increase dramatically during the summer as a result of solar energy absorption. Achieving and maintaining high average-volume temperatures inside the tubes may be more difficult in winter, when ambient average-volume temperatures are lower. The heat gathered by the tubes may require less supplemental heating in summer, when average volume temperatures are already warm, to attain the appropriate output average volume temperature for certain uses, such as producing hot water or space heating. In contrast, it may require more energy during the cold winter months to raise the average volume temperature inside the tubes to the desired level. Because some average winter volume temperatures can fall below freezing, the solar evacuated tubes may freeze. This risk may affect the system's operation and design. To avoid freezing-related damage, drain-back systems or antifreeze chemicals may be required. Some solar thermal systems may include adjustable components to enhance performance across different seasons or environmental conditions. For example, tracking devices can be used to more closely track the sun's motion , thereby maximizing the angle of incidence for solar energy, particularly during the winter months when the sun is higher. Some solar thermal systems allow storage of excess heat produced in summer for use in winter. Variations in average volume temperature throughout the year can affect the capacity and design of heat storage systems. In conclusion, seasonal fluctuations in solar radiation intensity and ambient conditions significantly influence the average temperature within the volume of solar evacuated tubes. Design considerations, system modifications, and component selection can all help solar thermal systems operate as efficiently as possible year-round while mitigating some seasonal issues.

Figure 8 shows a seasonal study of the evacuated-tube solar collector with an enclosure. The winter average volume temperature reached 304 K, while the summer average reached 314 K, which is reasonable given the change in winter climatic conditions.

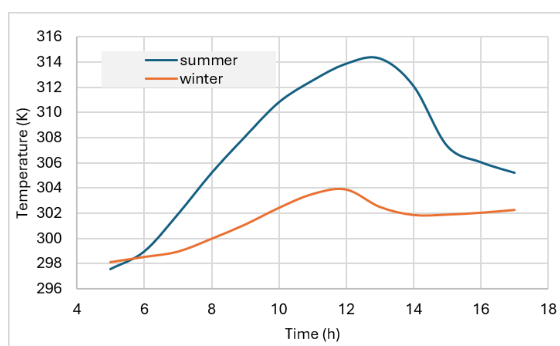

Figure 8. Average volume temperature gradient by using enclosure and 10 cm space in 0-azimuth degree at different seasons

Figure 9 shows the average volume temperature distribution across seasons. Despite the low average volume temperature in winter, the air had sufficient time to heat up so as to surround the vacuum tubes in the solar collector.

Figure 9 shows the average volumetric temperature in the enclosure with a 10 cm air space in front and at a 0° azimuth during different seasons: (a) summer and (b) winter. They demonstrate the influence of seasons on heat accumulation within the system. During summer, intense direct sunlight causes the heater in Figure 9a to raise the enclosure's internal temperature to approximately 314 K. When it's winter (Figure 9b), the temperature drops to around 304 K since the sun is less intense and shines for only a short time each day. In winter, less external heating may be required because of the enclosed design; nonetheless, it operates effectively and maintains good thermal performance. It clearly demonstrates how the enclosure maintains a stable internal temperature despite seasonal changes.

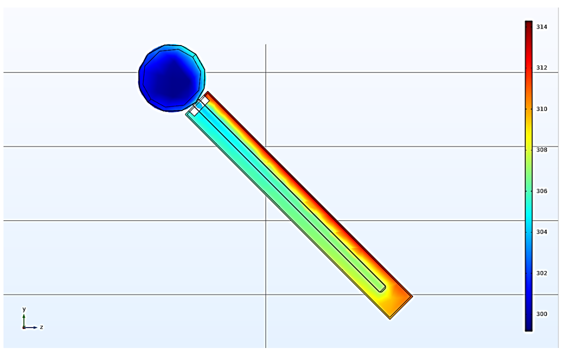

(a)

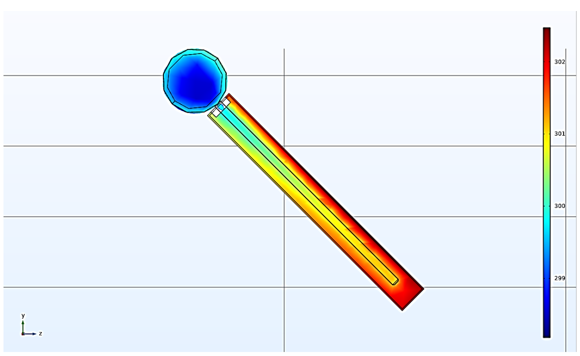

(b)

Figure 9. Average volume temperature contour using an enclosure and 10 cm spacing at 0° azimuth for different seasons: **(a)** July (summer) and **(b)** February (winter)

3.4. Thermal efficiency

The thermal efficiency of a solar thermal system depends on the width of the enclosure. Figure 10 shows the thermal efficiency over time. Thermal efficiency increases to 94.29% when the enclosure is used at 1 p.m. and at a distance of 10 cm. At 20 cm, it reaches 94.25%; at 30 cm, it decreases to 94.18%. As for the hours after noon, it was noticed that the enclosure retains heat inside itself and gives it to the pipes, and this gives an advantage in the case of charging the pipes during times when the sun sets due to the hot air inside the enclosure. Figure 11 shows the effect of the azimuth angle on solar vacuum tubes. The angle of 0 degrees received more solar radiation (94.29%) than the angle of 40 degrees (94.14%). It also increases thermal efficiency during extended hours. Figure 12 presents a seasonal study of the evacuated-tube solar collector fitted with an enclosure. The winter thermal efficiency reached 91.1%, and the summer efficiency reached 94.29%; these values correspond to a reasonable average volume temperature in relation to the change in winter climatic conditions.

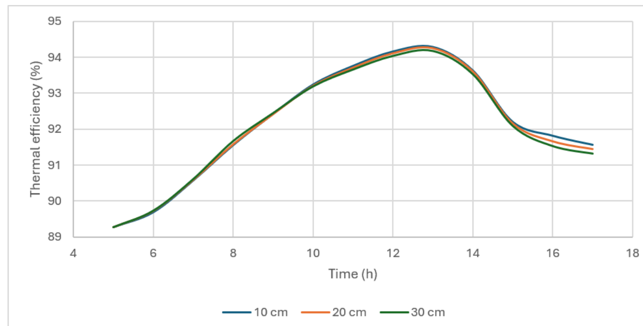

Figure 10. Thermal efficiency gradient using enclosure at different space in summer and azimuth 0 degree

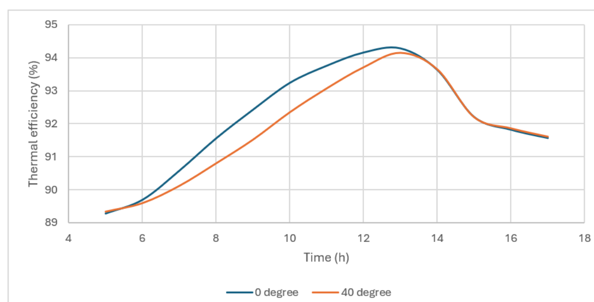

Figure 11. Thermal efficiency gradient by using enclosure and 10 cm space in summer at different azimuth degree

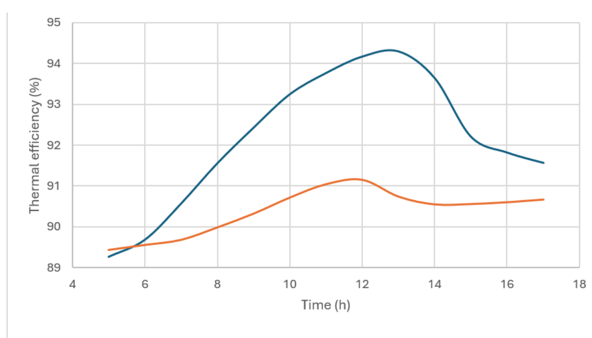

Figure 12. Thermal efficiency gradient by using enclosure and 10 cm space in 0-azimuth degree at different seasons

The enclosure method used in this study reduces environmental heat loss by forming a passive insulating barrier around evacuated tubes, without affecting flow within the tubes or requiring any supplementary energy input. The enclosure approach stands out because it combines simplicity of materials, low installation costs, scalability, and ease of application to solar systems that require no additional energy input. This distinguishes it from magnetic-field-dependent or nanofluid stability approaches (Zhang et al., 2018; Liu et al., 2020; Wang et al., 2019). The temperature increase reached 328 K using a method that exceeded previous research findings of 321 K, while preserving operational ease and mechanical stability across different climate zones (see Table 5).

Table 5. Summary of thermal efficiency and temperature vs. Enclosure size, azimuth, and season

Condition	Enclosure Gap (cm)	Azimuth Angle (°)	Season	Avg. Temp (K)	Thermal Efficiency (%)	Figure Ref.
Enclosure gap comparison	10	0	Summer	314.5	94.29	Fig. 4, Fig. 5a
	20	0	Summer	314.0	94.25	Fig. 5b
	30	0	Summer	~312.0	94.18	Fig. 5c
Azimuth angle comparison (10 cm gap)	10	0	Summer	314.5	94.29	Fig. 6, Fig. 7a
	10	40	Summer	313.0	94.14	Fig. 6, Fig. 7b
Seasonal comparison (10 cm, 0° azimuth)	10	0	Summer	314.0	94.29	Fig. 8, Fig. 9a
	10	0	Winter	304.0	91.10	Fig. 8, Fig. 9b
Maximum recorded temperature	—	—	—	328.0	—	Fig. 13b

An enclosure gap of 10 cm proved thermally optimal compared with the others because of (a) radiation trapping and (b) extensive convective loss. The air layer within the enclosure at this spacing will be narrow enough to minimize natural convection currents, thereby reducing heat loss due to air movement. At the same time, the proximity of the front glass enhances the trapping and re-radiation of solar radiation incident on the glass of the evacuated tube. Greater airflow increases convective heat transfer; a 20-30 cm gap reduces the enclosure's insulating effect. Therefore, the 10-cm gap strikes a balance between insulation and the high rate of solar energy absorption and convective flow.

From a cost–benefit perspective, a passive enclosure system is cost-effective and requires minimal maintenance aimed at enhancing the performance of the solar collector. The average price of a typical passive enclosure of glass and coated steel is approximately 30 to 50 dollars a square meter. By comparison, the cost of installation of reflective concentrators or solar tracking systems is between 150 and 300 dollars per square meter and may entail additional energy for propulsion and maintenance. Although reflectors and trackers can somewhat improve energy acquisition (usually 5-15 percent), they increase mechanical complexity and operating costs. By comparison, the passive enclosure improved thermal efficiency by as much as 7 K (328 K max) and operated in energy-free or mechanically weak areas, since the enclosure provided 94.29 percent thermal efficiency. Enclosures are also attractive in the design of long-term sustainable systems because of their ease of operation and long-term dependability.

3.5. Sensitivity analysis insights

The performance of the solar evacuated-tube collector is most affected by seasonal variation. With the enclosure gap and the azimuth angle kept constant, the average internal temperature will decrease by about 10 K when transitioning from summer to winter. Moreover, the thermal efficiency decreases by over 3 percent. A large change indicates that environmental conditions surrounding the system, such as solar irradiance and air temperature, have a significant influence on the thermal performance of the system. Thus, consistent year-round operation requires optimizing the system for seasonal differences, potentially through phase-change materials or heat storage. The second most influential factor is the azimuth angle, which determines the orientation of the solar collector relative to the sun's apparent motion. Shifting the orientation from 0 to 40 degrees, while keeping the same enclosure and seasonal temperature, causes the mean temperature to decrease by nearly 1.5 K and the thermal efficiency to decline by 0.15 percent. Although this variation is not as dramatic as the variation caused by seasonal changes, it shows that when the collector is oriented incorrectly relative to solar radiation, its effectiveness at absorbing heat is reduced. Therefore, during installation, an appropriate orientation should be selected to maximize energy production. The enclosure gap is among the parameters that significantly affect performance. When the clearance between the evacuated tubes and the enclosure walls is increased from 10 cm to 30 cm, the drops in temperature and thermal efficiency are rounded to 2.5 K and 0.11 percent, respectively. Although this effect is pronounced, it can nevertheless play a significant role in providing thermal insulation. This reduces convective heat loss by improving heat entrapment through a reduced gap. Hence, the optimum enclosure gap, based on insulation and the simplicity of the system, is 10 cm (see Tables 6–10).

Table 6. Sensitivity parameters and ranges

Parameter	Values Analyzed	Description
Enclosure Gap	10 cm, 20 cm, 30 cm	Space between enclosure walls and vacuum tubes
Azimuth Angle	0°, 40°	Orientation of collector relative to solar direction
Season	Summer (July), Winter (Feb)	Different ambient temperatures and solar intensities

Table 7. Summary of sensitivity results

Condition	Avg. Temp (K)	Thermal Efficiency (%)	ΔT vs. Baseline (321 K)	Δη vs. Max (%)
Gap 10 cm, 0° Azimuth, Summer	314.5	94.29	+7.5	0.00 (max)
Gap 20 cm, 0° Azimuth, Summer	314.0	94.25	+7.0	-0.04
Gap 30 cm, 0° Azimuth, Summer	~312.0	94.18	+5.0	-0.11
Gap 10 cm, 40° Azimuth, Summer	313.0	94.14	+6.0	-0.15
Gap 10 cm, 0° Azimuth, Winter	304.0	91.10	-17.0	-3.19
Max Recorded Temp	328.0	Not Specified	+7.0 vs. 321	—

Table 8. Sensitivity coefficients

Parameter	Sensitivity Coefficient (Temp)	Sensitivity Coefficient (Efficiency)
Enclosure Gap	~-1.25 K per 10 cm	~-0.055% per 10 cm
Azimuth Angle	~-0.1 K/°	~-0.0075%/°
Season Change	~-10.0 K	~-3.2%

Table 9. Estimated 95% confidence intervals(based on ±2σ)

Condition	Mean Temp (K)	CI (± 2σ)	95% CI Range (K)
Summer, 10 cm gap, 0° azimuth	314.5	±2.0	312.5 – 316.5
Summer, 20 cm gap, 0° azimuth	314.0	±2.0	312.0 – 316.0
Summer, 30 cm gap, 0° azimuth	~312.0	±2.0	310.0 – 314.0
Summer, 10 cm gap, 40° azimuth	313.0	±2.0	311.0 – 315.0
Winter, 10 cm gap, 0° azimuth	304.0	±2.0	302.0 – 306.0

Table 10. Mean thermal efficiency and confidence intervals for different enclosure gap sizes and azimuth angles

Condition	Mean Efficiency (%)	CI (± 2σ)	95% CI Range (%)
Summer, 10 cm gap, 0° azimuth	94.29	±0.50	93.79 – 94.79
Summer, 20 cm gap, 0° azimuth	94.25	±0.50	93.75 – 94.75
Summer, 30 cm gap, 0° azimuth	94.18	±0.50	93.68 – 94.68
Summer, 10 cm gap, 40° azimuth	94.14	±0.50	93.64 – 94.64
Winter, 10 cm gap, 0° azimuth	91.10	±0.50	90.60 – 91.60

3.6. Validation with previous research

The enclosure technique presented here offers practical advantages over other enhancement approaches reported in the literature. Previous investigations by Rahman et al. (2022), Li et al. (2021), and Khan et al. (2020) conducted studies on square-size vanes within porous media and porous cavities with vanes for Nusselt distribution and thermal analysis of MHD ferrofluid flow around cylindrical barriers through internal modifications of fluid cavities to enhance heat transfer. The research conducted by Wang et al. (2019) studied triangle cavities with barriers under buoyancy-driven nanofluid flow conditions (Wang et al., 2019), while Zhang et al. (2018) analyzed wavy porous cavities under magnetic field influence (Zhang et al., 2018) to achieve enhanced performance results. The implementations lead to effective results but concurrently require complex materials, active control systems, and intricate designs, which result in higher system expenses and greater complexity.

The similarity study we carried out with previous research by Sadeghi et al. (2020) [4] showed the role of implementing insulation in enhancing a house's hotness. Consistency is ensured in the simulation program by applying the same features, sizes, and details used previously through the addition of the enclosure to the process. A simulation of average volume temperature was carried out in accordance with the latest research, heating the pipe to 321 K based on prior simulations. In contrast, by incorporating the enclosure (Figure 13), the temperatures in this work are consistently 328 K or higher, which represents a clear advancement relative to the research paper that investigated the idea.

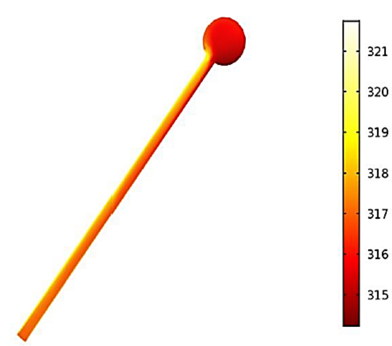

(a)

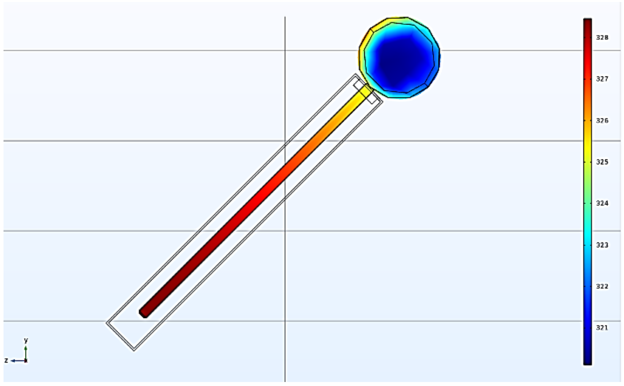

(b)

Figure 13. Average volume temperature profile of the ETSC water heater with 26 Lit tank capacity: **(a)** Sadeghi et al. work (2020) [4] and **(b)** present work

The effectiveness of using enclosures in the workplace has been demonstrated in comparative research, not only in terms of average volume temperature but also as a mechanism for improving thermal efficiency and saving energy. As in previous research, results were not comparable to those obtained in the current work due to the enclosure used, which led to a reduction in thermal energy. Figure 14 shows the difference in water temperatures in the solar collector without additives and provides a comparison with previous research, indicating close agreement (8.97% error) between temperature values.

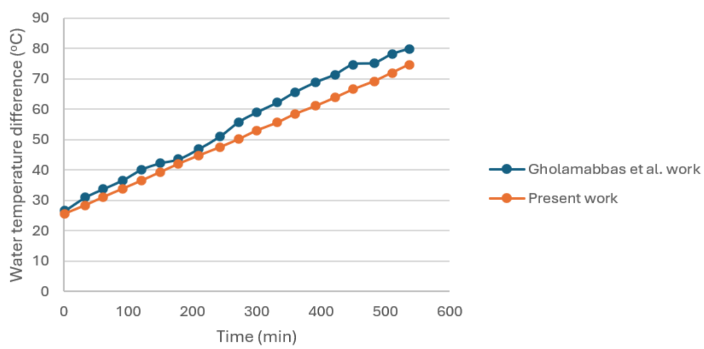

Figure 14. Verification of the numerical investigations of the ETSC water heater studies

The 7 K rise in temperature (321 K to 328 K) indicates how the external enclosure helps minimize heat losses from the solar evacuated-tube collector. This enhancement is due primarily to the enclosure's ability to reduce convective and radiative heat loss to the surroundings. The enclosure traps more solar energy by creating a controlled microclimate around the tubes through the glass front and insulated back wall, leading to increased internal temperatures. This simple passive technique can significantly improve the thermal performance without involving complicated materials or active systems.

The enclosure system presented shows considerable potential for low-cost, sustainable heating systems, particularly in environments that have varying conditions, i.e., different temperatures, humidity, and wind exposure. Compared with conventional improvement techniques that use nanofluids, active tracking systems, or internal structural alterations, this passive enclosure retains heat using common materials (glass and coated steel). The outcome is an increase in the average volume temperature by 1 K, to 328 K and a maximum thermal efficiency of 94.29%, both attained without any input of energy or operational complexity. This method is particularly valuable for off-grid rural systems, areas with limited economic development, small commercial and residential applications, and regions with large seasonal variability. This enclosure will retain heat during non-solar hours, making the system reliable for space heating and domestic hot water. Its low cost and ease of construction mean that it can be replicated in both urban and remote locations, where cost and energy efficiency are paramount; see Table 10.

Table 10. Summary of simulation results for solar evacuated tube collector performance

Parameter	Enclosure Gap	Azimuth Angle	Season	Max Avg. Tube Temp. (K)	Thermal Efficiency (%)
Optimal Setup	10 cm	0°	Summer	314.5	94.29
Enclosure gap variation	20 cm	0°	Summer	314.0	94.25
	30 cm	0°	Summer	312.0	94.18
Azimuth angle variation	10 cm	40°	Summer	313.0	94.14
Seasonal variation	10 cm	0°	Winter	304.0	91.10
Maximum recorded temperature	—	—	—	328.0 (peak condition)	—

3.7. Thermal inertia and long-term performance implications

A solar evacuated-tube collector with an external enclosure offers several benefits, including thermal inertia and extended service life. This aspect of the system—storing heat and releasing it slowly over time— is especially welcome during periods of low radiation, i.e., early mornings, evenings, or under cloud cover. The thermal inertia can be influenced mainly by the enclosure materials and the air gap that surrounds the evacuated tubes. Other materials used for thermal mass may include glass on the front cover and coated steel on the back wall, since these materials can retain heat gains during peak radiation hours and slowly release them when solar energy input is scarce. This assists in maintaining a more consistent internal temperature in the system and performs better than solar heating when the sky is not clear or the system is not receiving much direct sunlight.

Another major benefit of the external enclosure is heat retention. In sunny states, the system accumulates heat and subsequently delays its release during periods of low radiation or at night. This aspect is especially significant for an off-grid or low-resource installation, where the energy available during periods of reduced sunlight is a key factor in the system's subsequent reliability. The surrounding environment also prevents rapid cooling of interior temperatures by reducing convective heat loss, which is particularly effective in cloudy weather.

Such long-term effects on the performance of the external enclosure include increased system stability, reduced need for regular heating support, increased operational time, enhanced long-term resilience, energy savings during adverse weather, and long-term energy storage. The enclosure's thermal mass will also increase the system's durability because it minimizes thermal cycling effects and thereby reduces material degradation from repeated thermal cycling. Moreover, the application of phase change material(PCM) incorporated into the enclosure system can enhance energy storage and long-term system efficiency, and, therefore, present an extremely accurate and economical solution to the solar thermal energy system in the region of changing solar irradiance.

4. Conclusion

This paper demonstrates that a simple, non-customized encapsulation around solar evacuated-tube collectors substantially increased their thermal performance by minimizing thermal losses to the surrounding environment. An air gap enclosure of 10 cm increased the average volume temperature to 328 K, compared to 321 K without an air gap enclosure. The maximum thermal efficiency realized under summer conditions was 94.29%. This was achieved and sustained without the need for sophisticated materials, active solar positioning, or extra energy input. The findings indicate that external enclosures are a cost-effective and convenient addition to solar thermal systems, particularly in environments with unpredictable conditions. Prospectively, research is needed on how phase change materials (PCMs) can be integrated into enclosure design. Therefore, PCMs enable greater system stability and energy availability during off-sun hours, because surplus thermal energy can be stored during the middle of the day, when solar irradiation reaches its peak, and released during periods of low solar irradiation. It can also increase the efficiency of solar capture over a broader portion of the day by combining the passive enclosure with adaptive or half-passive solar tracking systems, namely gravity-driven or thermally activated mechanisms that accommodate large ranges of solar angle (e.g., tropical, temperate, and polar latitudes). The approach is also promising across a wide variety of climatic zones and cities of residence. In cold or temperate climates, the enclosure may serve as a thermal shield against ambient cold temperatures and wind chill, enhancing winter performance. The small size and non-invasive character of the enclosure system would enable it to be modified into a rooftop or facade installation in urban environments where active tracking can be impractical due to high construction density. Subsequent analysis must evaluate the system'sthermal response to different geographical locations with variable humidity, wind, and irradiance. Finally, the durability of materials used in enclosures must be considered. Though glass has a high solar transmittance and is durable, it can degrade when exposed to UV light or become soiled, both of which significantly reduce its efficiency. The back wall is made of coated steel, which must be able to withstand thermal cycling and be resistant to corrosion. Further testing should involve accelerated aging, material fatigue testing, and assessment of maintenance requirements to certify the system's long-term, stable performance. Expanding this study to larger-scale field trials and economic lifecycle studies will provide essential information about implementation and scalability in the real world.

One limitation encountered is that not all physical phenomena can be simulated by the simulation program because it requires a supercomputer. Future studies will explore the following variables: different climatic conditions; the system's performance over a longer period; and the materials used for the enclosure.

The use of external enclosures reduces environmental heat loss, resulting in improved thermal performance of solar evacuated tube collectors at an affordable implementation cost. Thermal efficiency reached a maximum of 94.29%, accompanied by an internal temperature increase to 328 K , achieved through the use of an external enclosure under various seasonal and azimuthal conditions. The research provides meaningful information for engineers and scholars in solar energy, building services, HVAC, and thermal engineering who aim to develop sustainable heating systems using basic materials and passive systems.

The study reaches reliable conclusions demonstrating the extent to which the system performs better with an external enclosure. Using an enclosure raised the temperature to 328 K, increased system efficiency to 94.29%, and produced greater thermal stability during the evening, all without installing expensive or active systems. The data show that the enclosure enables the solar collector to maintain good performance under variations in the sun's path and across seasons.

In the future, field tests, material tests, and phase-change materials should be incorporated to enhance the insulation and design of the system. Developers should also investigate adaptive enclosure approaches to sun tracking and the extended operation of systems across various climatic zones. These renewable energy sources and PCMs can be adapted via co-integration with adaptive tracking technology to maximize efficiency and utilization. PCMs are capable of storing excess heat at midday and can be placed inside walls or panels with very little alteration. Adaptive solar-tracking technology provides improved irradiance throughout the day, and contemporary microcontrollers and low-power mechanical systems have facilitated integration in mid- to large-scale installations. Studying these technologies would increase energy production, help manage diverse weather conditions, and improve enclosure in alternative thermal plans.

Author contributions statement

Dheya Ghanim Mutasher: Conceptualization, methodology, software, formal analysis, investigation, data curation, visualization, writing – original draft, and project administration. Lina Jassim: Methodology, validation, formal analysis, and writing – review & editing. Ali Najim Abdullah Saieed: Validation, investigation, resources, and writing – review & editing. Karrar A. Hammoodi: Software, visualization, validation, and writing – review & editing. Hasan Shakir Majdi: Supervision, conceptualization, validation, project administration, and writing – review & editing. All authors read and approved the final manuscript.

Declaration of interests

The authors declare that they have no known competing financial interests or personal relationships that could have appeared to influence the work reported in this paper.

Data availability

The data that support the findings of this study are available from the corresponding author upon reasonable request.

Declaration of generative AI and AI-assisted technologies in the writing process

During the revision of this manuscript, the authors used OpenAI's ChatGPT solely to assist in drafting and refining the language of the mandatory declaration statements. After using this tool, the authors reviewed and edited the content as needed and take full responsibility for the content of the publication.

Nomenclature

A	Surface area (m^2)
T	Temperature (K (Kelvin))
T_i	Temperature of surface i (K)
T_j	Temperature of surface j (K)
σ	Stefan-Boltzmann constant ($W/m^2 \cdot K^4$)
ε	Emissivity of surface - (dimensionless)
Q	Heat transfer rate (radiation or convection) W (Watts)
h	Convective heat transfer coefficient ($W/m^2 \cdot K^4$)
ρ	Density (kg/m^3)
c_p	Specific heat capacity (J/kg-K)
k	Thermal conductivity ($W/m \cdot K$)
v	Velocity vector (m/s)
P	Pressure (Pa (Pascal))
μ	Dynamic viscosity (Pa-s)
Φ	Volumetric heat generation (W/m^2)
J_k	Radiosity of surface k (W/m^2)
E_k	Emissive power of surface k (W/m^2)
F_{ij}	View factor from surface i to surface j - (dimensionless)
η	Thermal efficiency (% or -)
$\dot{m}$	Mass flow rate (kg/s)
I	Solar irradiance (DNI/DHI) (W/m^2)
ΔT	Temperature difference (K)

References

[1] A. Nokhosteen, S. Sobhansarbandi, Numerical modeling and experimental cross-validation of a solar thermal collector through an innovative hybrid CFD model, Renew. Energy. 172 (2021) 918–928. https://doi.org/10.1016/j.renene.2021.03.070.

[2] V.R. Pawar, S. Sobhansarbandi, CFD modeling of a thermal energy storage based heat pipe evacuated tube solar collector, J. Energy Storage. 30 (2020) 101528. https://doi.org/10.1016/j.est.2020.101528.

[3] A. Yurddaş, Optimization and thermal performance of evacuated tube solar collector with various nanofluids, Int. J. Heat Mass Transf. 152 (2020) 119496. https://doi.org/10.1016/j.ijheatmasstransfer.2020.119496.

[4] G. Sadeghi, M. Najafzadeh, H. Safarzadeh, Utilizing Gene-Expression Programming in Modelling the Thermal Performance of Evacuated Tube Solar Collectors, J. Energy Storage. 30 (2020) 101546. https://doi.org/10.1016/j.est.2020.101546.

[5] J.J. Ramírez-Minguela, J.A. Alfaro-Ayala, V.H. Rangel-Hernández, A.R. Uribe-Ramírez, J.M. Mendoza-Miranda, V. Pérez-García, J.M. Belman-Flores, Comparison of the thermo-hydraulic performance and the entropy generation rate for two types of low temperature solar collectors using CFD, Sol. Energy. 166 (2018) 123–137. https://doi.org/10.1016/j.solener.2018.03.050.

[6] S. ed D. Fertahi, T. Bouhal, T. Kousksou, A. Jamil, A. Benbassou, Experimental study and CFD thermal assessment of horizontal hot water storage tank integrating Evacuated Tube Collectors with heat pipes, Sol. Energy. 170 (2018) 234–251. https://doi.org/10.1016/j.solener.2018.05.062.

[7] J.A. Alfaro-Ayala, O.A. López-Núñez, F.I. Gómez-Castro, J.J. Ramírez-Minguela, A.R. Uribe-Ramírez, J.M. Belman-Flores, S. Cano-Andrade, Optimization of a solar collector with evacuated tubes using the simulated annealing and computational fluid dynamics, Energy Convers. Manag. 166 (2018) 343–355. https://doi.org/10.1016/j.enconman.2018.04.039.

[8] T. Bouhal, S. ed D. Fertahi, Y. Agrouaz, T. El Rhafiki, Y. Zeraouli, A. Jamil, Towards an energy efficiency optimization of solar horizontal storage tanks and circulation pipes integrating evacuated tube collectors through CFD parametric studies, Sustain. Energy Technol. Assessments. 26 (2018) 93–104. https://doi.org/10.1016/j.seta.2017.10.004.

[9] R. Farjallah, M. Chaabane, H. Mhiri, P. Bournot, H. Dhaouadi, Thermal performance of the U-tube solar collector using computational fluid dynamics simulation, J. Sol. Energy Eng. Trans. ASME. 138 (2016) 1–8. https://doi.org/10.1115/1.4034517.

[10] J.A. Alfaro-Ayala, G. Martínez-Rodríguez, M. Picón-Núñez, A.R. Uribe-Ramírez, A. Gallegos-Muñoz, Numerical study of a low temperature water-in-glass evacuated tube solar collector, Energy Convers. Manag. 94 (2015) 472–481. https://doi.org/10.1016/j.enconman.2015.01.091.

[11] L.A. Tagliafico, F. Scarpa, M. De Rosa, Dynamic thermal models and CFD analysis for flat-plate thermal solar collectors - A review, Renew. Sustain. Energy Rev. 30 (2014) 526–537. https://doi.org/10.1016/j.rser.2013.10.023.

[12] A.W. Badar, R. Buchholz, Y. Lou, F. Ziegler, CFD based analysis of flow distribution in a coaxial vacuum tube solar collector with laminar flow conditions, Int. J. Energy Environ. Eng. 3 (2012) 1–15. https://doi.org/10.1186/2251-6832-3-24.

[13] A.I. Sato, V.L. Scalon, A. Padilha, Numerical analysis of a modified evacuated tubes solar collector, Renew. Energy Power Qual. J. 1 (2012) 384–389. https://doi.org/10.24084/repqj10.322.

[14] M. Hayek, Investigation of evacuated-tube solar collectors performance using computational fluid dynamics, 2009 Int. Conf. Adv. Comput. Tools Eng. Appl. ACTEA 2009. (2009) 240–244. https://doi.org/10.1109/ACTEA.2009.5227901.

[15] L.J. Shah, S. Furbo, Theoretical flow investigations of an all glass evacuated tubular collector, Sol. Energy. 81 (2007) 822–828. https://doi.org/10.1016/j.solener.2006.09.007.

[16] L.E. Juanicó, Modified vacuum tubes for overheating limitation of solar collectors: A dynamical modeling approach, Sol. Energy. 171 (2018) 804–810. https://doi.org/10.1016/j.solener.2018.07.021.

[17] S. Yan, F. Wang, Z.G. Shi, R. Tian, Heat transfer property of SiO2/water nanofluid flow inside solar collector vacuum tubes, Appl. Therm. Eng. 118 (2017) 385–391. https://doi.org/10.1016/j.applthermaleng.2017.02.108.

[18] C. Lamnatou, C. Cristofari, D. Chemisana, J.L. Canaletti, Building-integrated solar thermal systems based on vacuum-tube technology: Critical factors focusing on life-cycle environmental profile, Renew. Sustain. Energy Rev. 65 (2016) 1199–1215. https://doi.org/10.1016/j.rser.2016.07.030.

[19] X. Li, Y.J. Dai, Y. Li, R.Z. Wang, Performance investigation on a novel single-pass evacuated tube with a symmetrical compound parabolic concentrator, Sol. Energy. 98 (2013) 275–289. https://doi.org/10.1016/j.solener.2013.10.015.

[20] T. Sultana, G. Morrison, R. Taylor, Performance of a Linear Fresnel Rooftop Mounted Concentrating Solar Collector, Aust. Sol. Energy Soc. Annu. Conf.(2012)6–7. https://www.researchgate.net/publication/306199843_Performance_of_a_linear_fresnel_rooftop_mounted_concentrating_solar_collector.

[21] J. Facão, A.C. Oliveira, Numerical simulation of a trapezoidal cavity receiver for a linear Fresnel solar collector concentrator, Renew. Energy. 36 (2011) 90–96. https://doi.org/10.1016/j.renene.2010.06.003.

[22] R. Capelli, G. Pozzi, A bridge between two important problems in optics and electrostatics, Eur. J. Phys. 29 (2008) 927–935. https://doi.org/10.1088/0143-0807/29/5/006.

[23] Roshani, H., Jalili, B., Mirzaei, A., Jalili, P., & Domiri Ganji, D. (2024). The effect of buoyancy force on natural convection heat transfer of nanofluid flow in triangular cavity with different barriers. Heliyon, 10, e35690. https://doi.org/10.1016/j.heliyon.2024.e35690.

[24] Jalili, B., Bahmani, M., Jalili, P., Liu, D., Alderremy, A. A., Domiri Ganji, D., & Vivas-Cortez, M. (2025). Investigating the influence of square size vanes on heat transfer in porous media: an in-depth Nusselt distribution. Journal of Computational Design and Engineering, 12, 1–14. https://doi.org/10.1093/jcde/qwae096.

[25] Bahmani, M., Babagoli, M., Jalili, P., Jalili, B., & Domiri Ganji, D. (2024). Numerical study of the porous cavity with different square size vanes with a high focus on Nusselt number. International Journal of Thermofluids, 24, 100860. https://doi.org/10.1016/j.ijft.2024.100860.

[26] Mirzaei, A., Jalili, B., Jalili, P., & Domiri Ganji, D. (2024). Free convection in a square wavy porous cavity with partly magnetic field: a numerical investigation. Scientific Reports, 14, 14152. https://doi.org/10.1038/s41598-024-64850-7.

[27] Jalili, B., Emad, M., Hasani Malekshah, E., Jalili, P., Akgül, A., & Hassani, M. K. (2024). Investigating double-diffusive natural convection in a sloped dual-layered homogenous porous-fluid square cavity. Scientific Reports, 14, 7193. https://doi.org/10.1038/s41598-024-57395-2.

[28] “Products.” GetX, www.getx.ca/products/. Accessed 25 May 2023.